

# *In-silico* Virtual Screening and ADMET Study to Find Novel Neuraminidase N1 Inhibitors Extended to the 150-Cavity

Ashraf Ahmed Ali Abdalsalam\*

Department of Pharmaceutical Chemistry, Faculty of Pharmacy, University of Sebha, Sebha, Libya.

---

## ARTICLE INFO

### Article history:

Received on: 02/03/2017

Accepted on: 24/04/2017

Available online: 30/05/2017

### Key words:

Virtual screening; H1N1; Oseltamivir; Neuraminidase inhibitor; ZINC database.

---

## ABSTRACT

Neuraminidase (NA) is the major surface protein of the influenza virus. It extracellularly acts by cleaving the terminal neuraminic acid from cellular receptors recognized by the Hemagglutinin. Then, it facilitates the release of newly formed viruses from the host cell surface to the neighboring cells, thereby facilitating the spread of the virus. A 150-cavity adjacent to the active conservative site is possessed by the group-1 neuraminidase, thereby rendering conformational change from open to close form when the ligand binds to the enzyme. In the present study, author reported an *in silico* virtual screening and docking analysis for potential neuraminidase inhibitors of various ligands obtained from the ZINC database using Autodock Vina against the 3TI6 protein. Analysis of 850 screened ligands reveal that five compounds with free binding energies of -11.2, -10.9, -10.4, -10.4, and -10.1 kcal/mol (ZINC03260201, ZINC09153352, ZINC09460395, ZINC13128611, and ZINC20605436, respectively) showed interaction with the protein at the known active site, as well as with the 150-cavity creating a stronger interaction between the ligand and the protein. Furthermore, lower binding energy is exhibited compared with the co-crystallized drug oseltamivir. *In silico* absorption, distribution, metabolism, and excretion (ADMET) prediction revealed that best compounds show comparative results with oseltamivir. Novel compounds interacting with the 150-cavity were successfully identified using this approach; such compounds could serve as a potential lead compound for developing a new anti-neuraminidase drug.

---

## INTRODUCTION

Influenza A virus is considered a serious health problem because of the annual morbidity and mortality caused by this disease (Couch *et al.*, 1996). Influenza virus, which belongs to the family of Orthomyxoviridae is subdivided into three different types, namely, A, B, and C. Influenza A and B are considered pathogens to humans, thereby becoming a cause for concern; by contrast, the Type C appears to have no association with any important diseases (Webster *et al.*, 1993; Melagraki *et al.*, 2007). Two surface glycoproteins namely, hemagglutinin (HA) and neuraminidase (NA), are attached to the influenza virus. The role of hemagglutinin is to help the virus attach to and penetrate the host cell via sialic acid (SA) binding sites

(Couceiro *et al.*, 1993; Wileyand Skehel, 1987), whereas the neuraminidase (NA) role is to cleave terminal sialic acid residues between cleaved terminal sialic acid residues.

This finding mainly explained why NA is taken as a drug target for developing agents in influenza drug discovery. Given its role in cleaving SA residues on the cellular receptor, which bind to the newly formed virions, Influenza virus neuraminidase inhibitors (NAIs) have emerged as promising therapeutic agents for the treatment of influenza. Current treatment exists for influenza infections with the newer class of neuraminidase inhibitors, such as zanamivir (Relenza) and oseltamivir (Tamiflu) (Von Itzstein, 2007; Xu *et al.*, 2008).

Zanamivir and oseltamivir were active against NAs from Groups 1 and 2 Influenza A as well as Influenza B viruses (Collins *et al.*, 2008). *In-silico* drug discovery is considered one of the most promising methods used to accelerate the drug development process (Tollman *et al.*, 2001).

\* Corresponding Author

Ashraf Ahmed Ali Abdalsalam, Department of Pharmaceutical Chemistry, Faculty of Pharmacy, University of Sebha, Sebha, Libya.  
Email: [ash2006rf@yahoo.com](mailto:ash2006rf@yahoo.com)

Virtual screening (VS) is a method widely utilized in the field of drug discovery, where a different study showed successful application to find a potent drug (Oprea and Matter, 2008). In the past few years, many reports showed that the method of VS was successfully used in making qualitative predictions that showed the distinction between the active and inactive compounds against a specific target (Chen, 2008; Chang *et al.*, 2011; Lin *et al.*, 2011). The VS primarily aims to find an active compound against a particular protein from thousands of compounds present in the databases. Case studies were applied, and they proved that VS played a significant role leading to the discovery of compounds currently in the stage of clinical trial (Melagraki *et al.*, 2007; Gadhe *et al.*, 2010; Goodarzi *et al.*, 2010). Flexible loop (called 150-loop), as well as a cavity (known as 150-cavity), adjacent to the known conservative active site, are found in the group-I neuraminidase.

Once this loop and cavity bind with inhibitors, the conformational change from open to close form can be rendered by group-1 NAs, whereas group-2 neuraminidase undertakes a closed form at all times.

By using structural analysis the result showed that neuraminidase group-I (N1, N4, N5 and N8) have additional cavity (150-cavity) compare to the group-II neuraminidase. The location of the 150-cavity is adjacent to the main active site, between the two residues 147 and 152 of the 150-loop.

All well-known influenza neuraminidase contain a 150-loop that can be in one of two kinds of conformations: first one an open conformation that leads to form the 150-cavity and the second one a closed conformation, that leads to an active site without a 150-cavity. Considering the fact that changes from open to close form at the active site of group-I NAs when the inhibitor binding to the enzyme, this encouraging to study the conformational transformation that open insights to find specific inhibitor would be effective against the group-I NAs that can be used to inhibiting the NAs by the conservative active site as well as 150-cavity, simultaneously (Amro *et al.*, 2011; Li *et al.*, 2010) Different studies reported that all group-I neuraminidases having an open conformation and all group-II neuraminidases have a closed conformation (Xu *et al.*, 2008; Russell *et al.*, 2006).

In the present study virtual screening has been employed to identify potential neuraminidase inhibitors from ZINC database that could interact with the conservative binding site, as well as the 150-cavity in the N1 group neuraminidase.

## MATERIAL AND METHODS

### Preparation of receptor for virtual screening

The crystal structure of neuraminidase of influenza A virus in complex with oseltamivir (PDB ID: 3TI6) (Vavricka *et al.*, 2011), was obtained from Protein Data Bank ([www.rcsb.org](http://www.rcsb.org)), the crystal structure consist of two chains (A and B) where chain A was used. The co-factor and water molecules were removed and hydrogen were added using AutoDockTools (ADT).

### Ligands screening from ZINC database

The three dimensional structure of 850 ligand molecules were retrieved from ZINC database (Irwin and Shoichet, 2005) in mol2 format, then the ligands converted to pdbqt using raccoon (Forli *et al.*, 2016) to be used for virtual screening with AutoDock Vina.

### Molecular docking

The Autodock Vina was used to perform virtual screening, and all the needed file were prepared. The protein converted from pdb to pdbqt using ADT, The size of grid box with dimensional 25, 25, 25 for x, y, z coordinates in Å, where centered on the binding site of the enzyme; the ligand file converted from mol2 to pdbqt using raccoon. Confi.txt file created including all the necessary information needed to conduct the virtual screening. Other configurations were considered default.

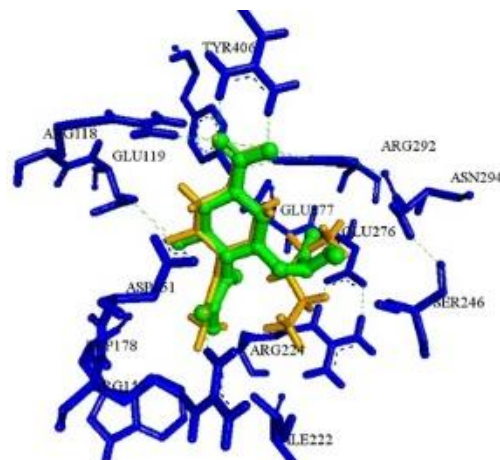
### Absorption, distribution, metabolism, excretion and toxicity (ADMET)

In this study absorption, distribution, metabolism, excretion and toxicity (ADMET) of the selected compounds were predicted using the ADMET SAR database (Cheng *et al.*, 2012). This database is known as a knowledge based tool that used for *In-silico* screening of the ADMET properties for all types of compounds.

## RESULTS AND DISCUSSION

### Validation of the docking protocol

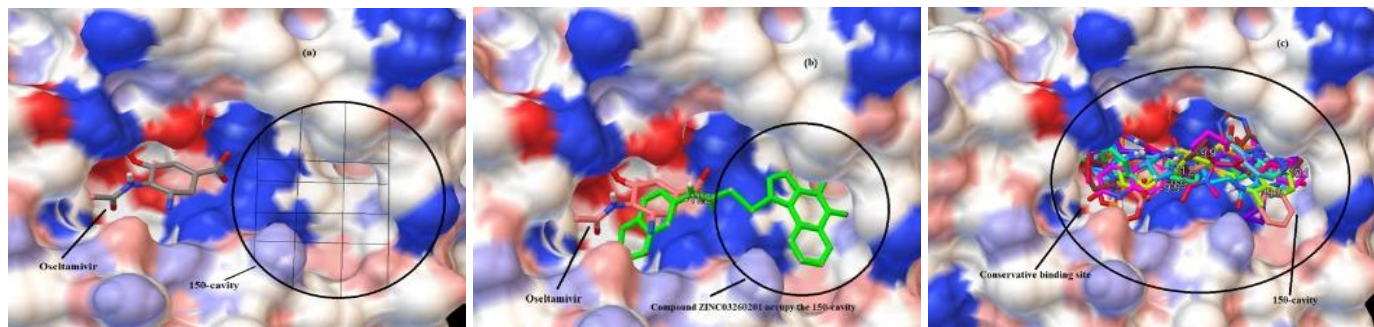
Before conducting the virtual screening of the selected ligand, control docking was conducted by re-docking the co-crystallized structure of neuraminidase in complex with oseltamivir (PDB:3TI6). The docking results showed that the binding conformation of re-docked oseltamivir reproduced the expected binding mode of the co-crystallized ligand. It showed binding affinity -6.6 kcal/mol, and the root mean square deviation (RMSD) was 1.47, as shown in Figure 1.



**Fig. 1:** The Superimposition between the docked conformation (yellow) and the crystal structure (green) of the Neuraminidase receptor-ligand complex of the H1N1 3TI6.

**Table 1:** Free energy of binding and the interactions between the best compounds and 3TI6.

No	Ligand	Binding energy $\Delta G$ (kcal/mol)	H-bonding	Van der Waals	Hydrophobic interaction	Pi-Alkyl	Pi-Cation
1	ZINC03260201	-11.2	Arg371, Arg371,Lys432, Ser370, Pro431	Trp640, Arg118, Asn347, Asn294, Glu227	Ile427, Asp151, Glu276, Asn294,Ser369	Lys432, Ile427, Pro431, Arg371,	Arg292
2	ZINC09153352	-10.9	Arg292, Arg371, Tyr406	Trp178,Asp151, Arg430,	,Arg152, Glu227, Arg118,Tyr406	Arg224, Ile222, Lys432, Trp403, Pro431	Arg118
3	ZINC09460395	-10.4	Arg292,Asn347, Arg371, Arg118,Tyr406	Glu276, Arg152	Glu227, Arg151, Trp406, Lys432	Ile427, Lys432,Trp403 Pro431	Glu277
4	ZINC13128611	-10.4	Arg371, Arg118, Arg292,	Arg430, Glu227, Arg152,Ser179	Gly429,Asp151, Ser179, Trp,178	Ile427, Lys432, Arg224Pro431	Asp151,
5	ZINC20605436	-10.1	Arg292, Glu227, Arg224	Asn294, Glu276,Arg 151, Glu119	Arg118,Glu276	Ile427, Lys432, Trp403, Ile222	Asp151, Arg371, Arg118
6	ZINC21877107	-10.1	Arg292, Arg118,	Glu227, Ser179, Ser179, Trp 178	Trp406,Asn347, Arg371, Tyr403,	Arg224, Trp403, Ile427, Pro341, Lys432	Asp151, Arg371
7	ZINC09430769	-9.9	Arg371, Arg371, Tyr406, Asp151, Ser246	Trp403,Asn294	Pro431, Arg118,Ser246, Arg224	Lys432, Ile427, Pro341	Arg292, Asp151
8	ZINC19753016	-9.9	Tyr406, Arg371, Arg292	Arg430, Arg118,Gly 429	Arg430, Pro431, Ile427, Asp151, Asn347	Pro341, Lys432, Arg371	Arg371
9	ZINC30714972	-9.9	Asp151,Arg371,Arg118, Trp406	Trp178,Ser179, Arg224, Arg292	Asp151,Trp178,Asn347 , Ile472, Trp403	Pro341, Lys432, Ile427,	Glu227, Arg152
10	ZINC05637343	-9.9	Asp151,Arg118,Arg371, Tyr406	Trp403, Gly429, Arg430	Arg224, Arg151, Glu227, pro431,Tyr406	Arg224, Lys432, Arg371, Pro341	Glu227
11	Oseltamivir	-6.5	Arg118, Arg292, Arg152, Arg371,Glu119	Tyr406, Asp151, Arg224, Glu276,	Glu119, Glu227, Ile222,		

**Fig. 2:** Panel (a) the standard drug oseltamivir in the conservative active site which adjacent to the 150-cavity of 3TI6. Panel (b) superposed of the oseltamivir with the best ligand. Panel (c) superposed of all the ten best ligands that occupy the 150-cavity.

### Analysis of interactions between ligand and receptor

All the 850 ligands chosen from the ZINC database were screened and docked within the binding pocket of the NA using Autodock Vina. Only those compounds with better binding affinities than oseltamivir were chosen. The binding pose of the selected compound was evaluated by comparing their types of interactions, hydrogen bonding, and interaction pattern with those of oseltamivir, as shown in (Table 1). A study using molecular dynamic simulation reveals that the pandemic 09N1 neuraminidase can exhibit the open 150-cavity conformations (Amaro *et al.*, 2011).

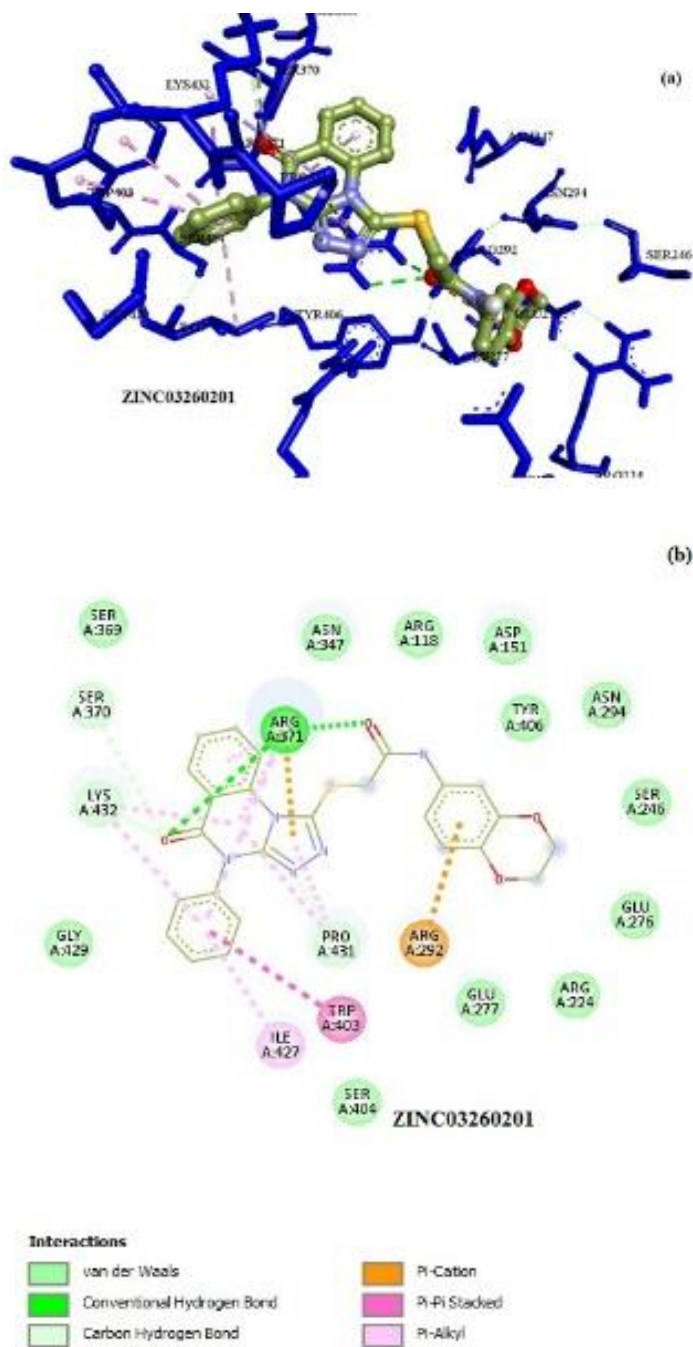
Figure 2 (a) shows a close view of the oseltamivir inside the binding pocket of the crystal structure of 3TI6. Adjacent to this pocket is the 150-cavity, where the cavity is vacant and no atom from the oseltamivir is attached to it. A comparison was made with

the best ligand. Analysis of the interactions between the top ten compounds from ZINC database and the target protein were found to be bonded deeply in the conservative pocket as well as to the adjacent 150-cavity that exhibiting both bonded and non-bonded interaction such as H-bond, van der Waals, hydrophobic,  $\pi$ -alkyl and  $\pi$ -cation,  $\pi$ - $\pi$  stacked interactions, Details of interactions as bellow.

ZINC03260201 occupying the known binding pocket as well as the 150-cavity (Fig.2 b). Superimposing of the best 10 compounds showed that all of them interact with amino acids in the 150-cavity (Fig.2c). The best compounds selected depend on the Lipinski role of five (Lipinski, 2004), where all the compounds have (i) MW less than 500, (ii) number of hydrogen donor less than 5, (iii) number of hydrogen acceptor less than 10, and (iv) logP less than 5 as shown in (Table 2).

**Table 2:** Drug-likeness properties of the best compounds.

NO	Zinc ID	logP	H-bond donors	H-bond acceptors	Molecular weight (g/mol)
1	ZINC03260201	3.93	1	9	485.525
2	ZINC09153352	4.23	1	8	473.625
3	ZINC09460395	3.75	1	6	431.536
4	ZINC13128611	3.62	0	7	478.618
5	ZINC20605436	3.71	2	8	477.999
6	ZINC21877107	2.18	2	9	475.549
7	ZINC09430769	2.27	1	7	437.521
8	ZINC19753016	2.40	1	6	428.56
9	ZINC30714972	3.42	1	6	437.525
10	ZINC05637343	4.46	2	7	408.385

**Fig. 3:** Panels (a) 3D, (b) 2D showed the ligand docked conformations of the ZINC03260201 within the conservative binding pocket and 150-cavity.

Discovery Studio Visualizer 4.0 software (Accelrys Inc., San Diego, CA) together with Ligplot (Wallace *et al.*, 1995) were used to analyze the detailed interaction of the best compounds that bind well to the active site with bonded and non-bonded interactions. These compounds showed lower binding energy than oseltamivir, thereby indicating a more favorable binding of these ligands at the active site of NA.

Through further investigation of the best compound, author found that the ZINC03260201 showed binding energy -11.2 kcal/mol and formed two conventional H-bond between oxygen of carbonyl groups and Arg371 and another carbon H-bond with Ser370 and Lys432 and Pro431. Pi ( $\pi$ )-cation interaction formed between the benzene ring and the Arg 292,  $\pi$ -alkyl interactions formed between the benzene

ring and Ile427 and Lys432 and between pentagonal ring and Pro431. Moreover, Trp403, Ile427, and Lys432 formed  $\pi$  -  $\pi$ stacked interactions. Asn347, Arg118, Asp 151, and Asn249 formed van der Waals interaction (Figure 3 a and b). Compound ZINC09153352 as second best compounds showed binding energy -10.9 kcal/mol and formed H-bonds between the oxygen in the carboxyl group and three amino acids Arg292, Arg371, and Tyr 406 and carbon H-bond with Glu227.

Arg371 and Arg118 formed three  $\pi$ - cation interaction with the benzene ring and pentagonal ring. Over six  $\pi$ -alkyl interactions were formed with Ile 222, Arg 224, Ile 427, Pro 431, Lys 432, and Trp 403. Van der Waals interaction was also shown with the amino acids Trp 178, Arg152, Glu 227, Asp 151, and Thr439 (Figure 4 a and b).

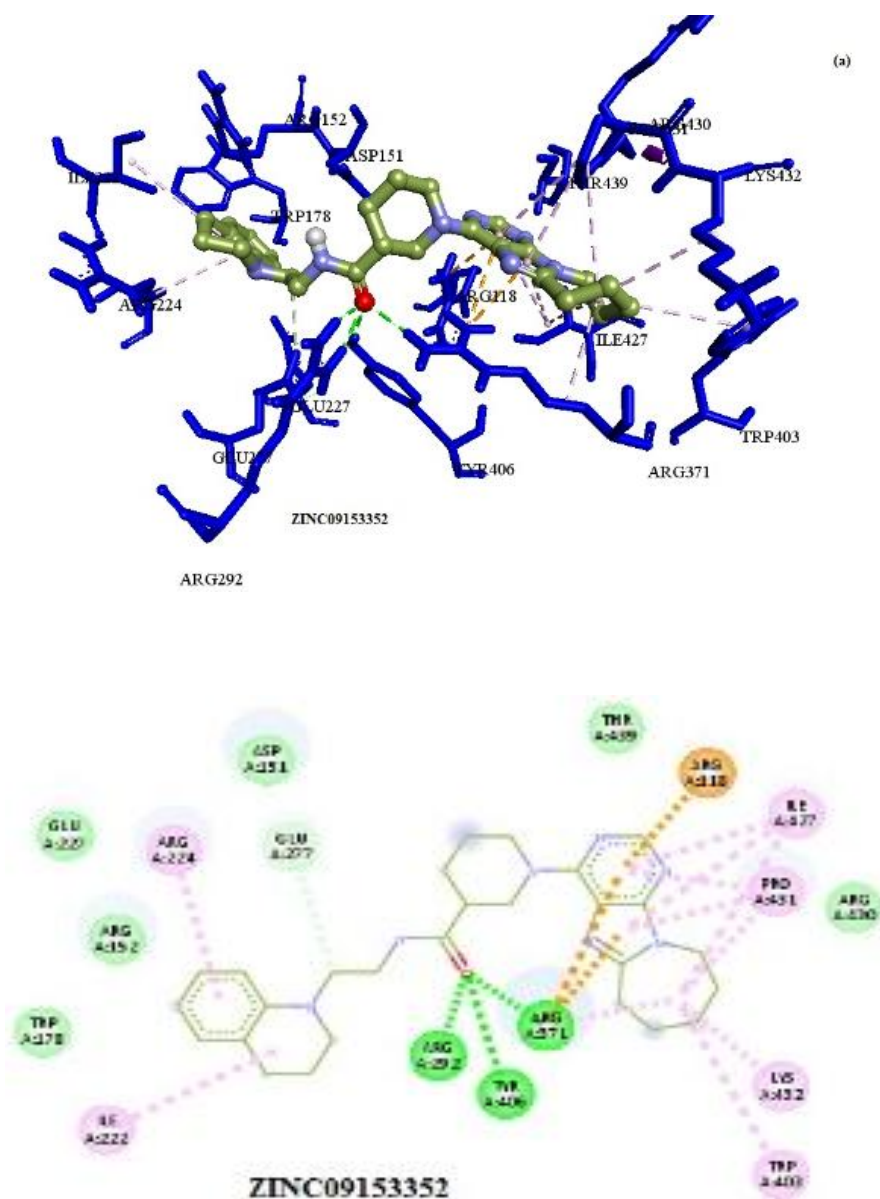


**Fig. 4:** Panels (a) 3D, (b) 2D showed the ligand docked conformations of the ZINC09153352 within the conservative binding pocket and 150-cavity.

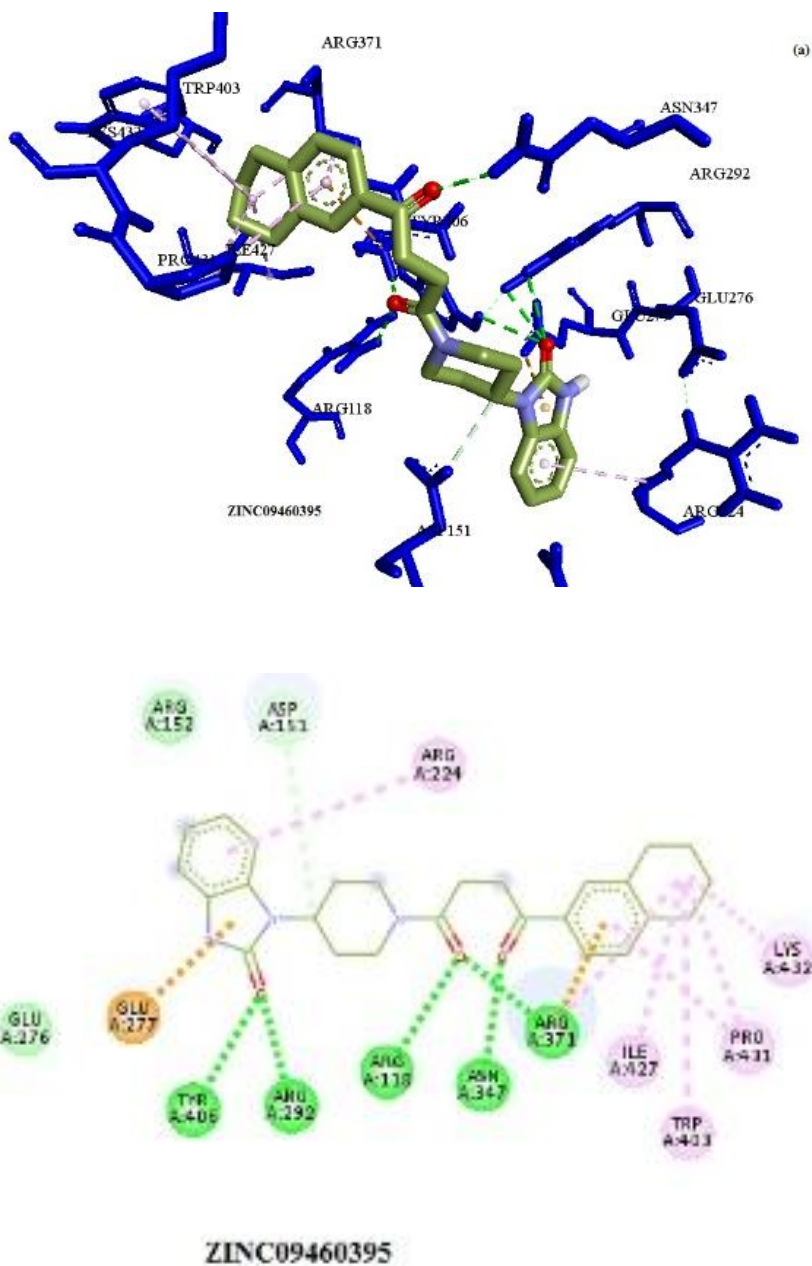


**Fig. 5:** Panels (a) 3D, (b) 2D showed the ligand docked conformations of the ZINC09460395 within the conservative binding pocket and 150-cavity.

Compound ZINC09460395 showed binding energy -10.4 kcal/mol and formed five conventional H-bonds with Tyr 406, Arg292, Arg118, Asn347, and Arg371 with oxygen in the carboxyl groups and the benzene ring.

Glu227 formed  $\pi$ -cation interaction with the pentagonal ring whereas Arg371 with the benzene ring. Another seven  $\pi$ -Alkyl interactions formed between Ile427, Pro431, Trp 403, Lys 432, Arg224, and Arg 371. Van der Waals interactions also formed with Glu276 and Arg152 (Figure 5 a and b).

Compound ZINC13128611 showed a binding energy of -10.4 kcal/mol and a different interaction with amino acids in the binding site. Conventional three hydrogens bonds between tried arginine Arg292, Arg118, Arg371 with the oxygen atom.  $\pi$ -cation formed between Asp151 amino acid and the benzene ring. Arg224, Pro431, Ile427, and Lys432 formed  $\pi$ -alkyl interaction with pentagonal and benzene rings, van der Waals interaction formed with Arh 178, Ser179, Glu227, Arg227, and Asn294 (Figure 6 a and b).



**Table 3:** Prediction of ADMET profile of the best compounds.

Model	ZINC03260201	ZINC09153352	ZINC09460395	ZINC13128611	ZINC20605436	Oseltamivir
Absorption						
Blood-brain barrier	BBB+	BBB+	BBB+	BBB+	BBB+	BBB-
Human intestinal absorption	HIA+	HIA+	HIA+	HIA+	HIA+	HIA-
Caco-2 permeability	Caco-2-	Caco-2-	Caco-2-	Caco-2-	Caco-2+	Caco-2-
Metabolism						
CYP450 2C9 substrate	Non-substrate	Non-substrate	Non-substrate	Non-substrate	Non-substrate	Non-substrate
CYP450 2D6 substrate	Non-substrate	Substrate	Non-substrate	Non-substrate	Non-substrate	Non-substrate
CYP450 3A4 substrate	Substrate	Substrate	Substrate	Substrate	Non-substrate	Substrate
CYP450 1A2 inhibitor	Non-inhibitor	Inhibitor	Non-inhibitor	Non-inhibitor	Non-inhibitor	Non-inhibitor
CYP450 2C9 inhibitor	Inhibitor	Non-inhibitor	Inhibitor	Inhibitor	Inhibitor	Non-inhibitor
CYP450 2D6 inhibitor	Non-inhibitor	Inhibitor	Non-inhibitor	Non-inhibitor	Non-inhibitor	Non-inhibitor
CYP450 2C19 inhibitor	Inhibitor	Inhibitor	Non-inhibitor	Inhibitor	Inhibitor	Non-inhibitor
CYP450 3A4 inhibitor	Inhibitor	Inhibitor	Inhibitor	Inhibitor	Inhibitor	Non-inhibitor
Toxicity						
AMES toxicity	AMES toxic	Non toxic	Non toxic	Non toxic	Non toxic	Non toxic
Carcinogens	Non-carcinogens	Non-carcinogens	Non-carcinogens	Non-carcinogens	Non-carcinogens	Non-carcinogens
Acute Oral Toxicity	III	III	III	III	III	

Compound ZINC20605436 showed binding energy -10.1 kcal/mol and formed three conventional H-bonds with Arg292, Arg224, and Glu227 and one carbon H-bond with Arg224. Four  $\pi$ -cation bonds formed with Arg371, Arg118, Asp151, and Glu227,  $\pi$ -alkyl interaction also formed with Ile222, Ile427, Trp403, Lys432, and Arg371. Arg430, Pro431, Glu119, Trp178, and Arg152 formed Van der Waals interaction (Figure 7 a and b).

Analysis of the virtual screening result showed that the best-selected ligand bound to the important residues in the conservative pocket, as well as with the residues in the 150-cavity Agr430, Thr439, Lys432, Ile427, Pro321, Trp304, Gly429, and Ser370, thereby exhibiting a difference for oseltamivir. The final poses for oseltamivir and the ten best compounds from Figure. 2 b interacted with the same amino acids in the conservative residues in the binding pocket similar to oseltamivir Asp151, Asp152, Arg192, and Arg371 Arg118.

Such finding is a result of the predicted free energy of the binding of these ligands, which interacted in a stronger manner with the target protein compared with oseltamivir. Furthermore, different types of interactions were exhibited by the best ligands. Hydrogen bonds with the tried arginine Arg118, Arg371, and Arg292 are important interactions in the conservative pocket, where most of the ligands form H-bonds with the same amino acids (Russell *et al.*, 2006). Hydrophobic and Van der Waals interactions also formed between the best ligands and the amino acid in the binding pocket Trp178, Tyr406, Lys432, Glu227, Trp406, Asn347, and Tyr403 and with the 150-cavity. Additional interactions, such as  $\pi$ -alkyl and  $\pi$ -cation with important residues, were exhibited only by the best ligands, oseltamivir failed to show any of these interactions. The mentioned interaction between the best ligands with the NA showed that the attachment of the compounds extended to the region of 150-cavity, thereby enhancing the binding affinity with the active site. From the above

mentioned observations, all the interactions created by the best compounds formed a stable complex between these compounds and NA active site and exhibited lower binding energy and expected strong inhibition *in vitro*.

#### ADME/T studies

Absorption, Distribution, Metabolism, Excretion, and Toxicity (ADMET) are important parameters for examining the drug-like properties of the molecules (Table 3). Depending on the virtual screening result, top ten potential ligands were submitted to the ADMET SAR web-server to generate an *in silico* pharmacokinetic parameter and determine the ADMET properties. All the selected ligands followed the Lipinski's rule of five. Considering this criterion, all the ligands are considered drug candidates for further ADMET study, with oseltamivir as the reference. The predicted ADMET descriptors include Caco-2 permeability, human intestinal absorption, blood brain barrier (BBB) penetration, P-glycoprotein substrate and inhibitor, CYP450 substrate and inhibitor, AMES mutagenicity, and carcinogens.

The absorption properties BBB, human intestinal absorption (HIA), and Caco-2 permeability demonstrating positive results confirm that all the compounds have no side effects on the absorption. For metabolism, most of the compound non-substrates for CYP450 2D6, except ZINC09153352, act as a substrate for CYP450 3A4; all the ligand substrates, together with oseltamivir, except ZINC20605436, were non-substrates; all the ligands are predicted as non-inhibitors for CYP450 2D6, except ZINC09153352. Furthermore, CYP450 3A4 is predicted as an inhibitor compared with oseltamivir, which is predicted as a non-inhibitor. Under toxic conditions, all the ligands are non-AMES toxic and non-carcinogenic, except ZINC03260201, which was AMES toxic.

## CONCLUSION

In the process of drug discovery, the method of virtual screening is used to reduce the time and cost. In this study, virtual screening was utilized to find better inhibitors from the ZINC database than the existing drug oseltamivir. These selected ligands were docked to the binding pocket of NA, where different types of interactions formed with the important amino acids in the conservative active site as well as the 150-cavity. These ligands showed binding affinities stronger than oseltamivir, with the best ligands having the capacity to accommodate the 150-cavity. Analysis of the molecular interactions for the best ligands reveals that ZINC03260201, ZINC09153352, ZINC09460395, ZINC13128611, and ZINC20605436 have favorable interactions with the important amino acids at the binding site, as well as with the 150-cavity of the neuraminidase enzyme compared with oseltamivir, which only binds to the conservative binding pocket. The top docking hits ZINC03260201, ZINC09153352, ZINC09460395, ZINC13128611, ZINC20605436 resulting from this study does not violate the Lipinski rule of five that can be taken as an orally active drug. *In-silico* ADMET studies further evaluating the ligands reveal that the best ligands have comparable pharmacological parameters to oseltamivir. The best ligands showed non-carcinogenic and non-toxic qualities, except one ligand showing AMES toxic. From ADMET study, valuable information could help improve the structure of the compounds as a drug candidate.

Therefore, this study shows the importance of this hypothesis in the screening of small molecule libraries, and the best compound could be used as a drug candidate and act as potent NA inhibitors.

## ACKNOWLEDGEMENTS

The author would like to thank staff members of Pharmaceutical Design and Simulation Laboratory (PhDs Lab), School of Pharmaceutical Sciences, University Sains Malaysia (USM).

**Financial support and sponsorship:** Nil.

**Conflict of Interests:** The authors' declare no conflict of interest.

## REFERENCES

Amaro RE, Swift RV, Votapka L, Li WW, Walker RC, Bush R.M. Mechanism of 150-cavity formation in influenza neuraminidase. *Nature*, 2011; 2:1-7.  
Available at: <http://www.accelrys.com> [Accessed 16 December 2016].  
Chang SS, Huang HJ, Chen CY. High performance screening, structural and molecular dynamics analysis to identify H1 inhibitors from TCM Database@Taiwan. *Mol Biosyst*, 2011; 7: 3366–3374.  
Chen CYC. Discovery of novel inhibitors for c-Met by virtual screening and pharmacophore analysis. *J Chin Inst Chem Eng*, 2008; 39:617–624.  
Cheng F, Li W, Zhou Y, Shen J, Wu Z, Liu G, Lee P, Tang Y. admetSAR: A Comprehensive Source and Free Tool for

Assessment of Chemical ADMET Properties. *J ChemInf Model*, 2012; 52:3099-3105.

Collins PJ, Haire LF, Lin LY, Liu J, Russell RJ, Walker PA, Skehel JJ, Martin SR, Hay AJ, Gamblin SJ. Crystal structures of oseltamivir-resistant influenza virus neuraminidase mutants. *Nature*, 2008; 453:1258-1261.

Couceiro JNSS, Paulson JC, Baum LG. Influenza virus strains selectively recognize sialy oligosaccharides on human respiratory epithelium, the role of the host cell in selection of hemagglutinin receptor specificity. *Virus Res*, 1993; 29:155-165.

Couch RB, Keitel W, Cate TR, Quarles JA., Taber LA, Glezen WP 1996. Prevention of influenza virus infections by current inactivated influenza virus vaccines. In *Options for the Control of Influenza III*, pp. 97–106. Edited by LE Brown, AW Hampson.

Forli S, Huey R, Pique ME, Sanner MF, Goodsell DS, Olson AJ. Computational protein-ligand docking and virtual drug screening with the AutoDock suite. *Nat Protoc*, 2016; 11:905-919.

Gadhe CG, Lee, SH, Madhavan T, Kothandan G, Choi D, Cho SJ. Ligand based CoMFA, CoMSIA and HQSAR analysis of CCR5 antagonists, *Bull Korean Chem Soc*, 2010; 31:2761-2770.

Goodarzi M, Freitas MP, Ghasemi N. QSAR studies of bioactivities of 1-(azacyclyl)3-arylsulfonyl-1H-pyrrolo[2,3-b]pyridines as 5-HT6 receptor ligands using physicochemical descriptors and MLR and ANN-modeling, *Eur J Med Chem*, 2010; 45:3911-3915.

Irwin JJ, Shoichet BK. ZINC – A Free Database of Commercially Available Compounds for Virtual Screening. *J ChemInf Model*, 2005; 45:177-182.

Li Q, Qi J, Zhang W, Vavricka CJ, Shi Y, Wei J, Feng E, Shen J, Chen J, Liu D, He J, Yan J, Liu H, Jiang H, Teng M, Li X, Gao GF. The 2009 pandemic H1N1 neuraminidase N1 lacks the 150-cavity in its active site. *Nat StructMol Bio*, 2010; 17:1266-1268.

Lin CH, Chang TT, Sun MF, Chen HY, Tsai FJ, Chang KL, Fisher M, Chen CY. Potent inhibitor design against H1N1 swine influenza: structure-based and molecular dynamics analysis for M2 inhibitors from traditional Chinese medicine database. *J BiomolStructDyn*, 2011;4: 471-482.

Lipinski CA. Lead- and drug-like compounds: the rule-of-five revolution. *Drug Discov Today Technol* 2004; 1:337-341.

Luo M. Structural biology: antiviral drugs fit for a purpose. *Nature*, 2006; 443:37-38.

Melagraki G, Afantitis A, Sarimveis H, Koutentis PA, Markopoulos J, Igglessi-Markopoulou O. A novel QSPR model for predicting  $\theta$  (lower critical solution temperature) in polymer solutions using molecular descriptors, *J Mol Model*, 2007; 13:55-64.

Mitrasinovic PM, On the structure-based design of novel inhibitors of H5N1 influenza A virus neuraminidase (NA). *BiophysChem*, 2009; 140:35-38.

Oprea TI, Matter H. Integrating virtual screening in lead discovery. *OpinChemBiol*, 2004; 8:349-358.

Russell RJ, Haire LF, Stevens DJ, Collins PJ, Lin YP, Blackburn GM, Hay AJ, Gamblin SJ, Skehel JJ. The structure of H5N1 avian influenza neuraminidase suggests new opportunities for drug design. *Nature*, 2006; 443:45-49.

Tollman P, Guy P, Altschuler J, Flanagan A, Steiner M, 2001. A Revolution in R&D: The Impact of Genomics. BCG Focus. The Boston Consulting Group, Boston, MA.

Vavricka CJ, Li Q, Wu Y, Qi J, Wang M, Liu Y, Gao F, Liu J, Feng E, He J, Wang J, Liu H, Jiang H, Gao GF. Crystal structure of 2009 pandemic H1N1 neuraminidase complexed with oseltamivir. *PLOS Pathogens*, 2010; 7:1002249.

Von Itzstein M. The war against influenza: discovery and development of sialidase inhibitors. *Nat Rev Drug Discov*, 2007; 6: 967-74.

Wallace AC, Laskowski RA, Thornton JM. LIGPLOT: a program to generate schematic diagrams of protein-ligand interactions. *Protein Eng*, 1995; 8:127-134.

Webster, RG. *et al.* 1993. in *Options for the Control of Influenza Virus II* (ed. Hannoun, C.) 177-185 (Excerpta Medica, Amsterdam).

Wiley DC, Skehel JJ. The structure and function of the hemagglutinin membrane glycoprotein of influenza virus, *Annu Rev Biochem*, 1987; 56:365-394.

Xu X, Zhu X, Dwek AR, James Stevens J, Wilson AL. Structural characterization of the 1918 influenza virus H1N1 neuraminidase. *J Virol*. 2008; 82:10493-10501.

**How to cite this article:**

Ashraf Ahmed Ali Abdalsalam., *In-silico* Virtual Screening and ADMET Study to Find Novel Neuraminidase N1 Inhibitors Extended to the 150-Cavity. *J App Pharm Sci*, 2017; 7 (05): 024-033